This is the accepted manuscript of the article: Zhu, Q., & Xiao, Q. (2024). Dynamics of seaweed-inspired piezoelectric plates for energy harvesting from oscillatory cross flow. Bioinspiration & Biomimetics, 19(4), Article 046004.
https://doi.org/10.1088/1748-3190/ad43d1

Dynamics of Seaweed-Inspired Piezoelectric Plates for Energy Harvesting from Oscillatory Cross Flow

Qiang Zhu[1]*and Qing Xiao[2]
[1]Department of Structural Engineering
University of California, San Diego, La Jolla, CA 92093, USA

[2]Department of Naval Architecture, Ocean and Marine Engineering
University of Strathclyde, Glasgow, G4 0LZ, Scotland, UK

March 19, 2024

Abstract

Inspired by the vibrations of aquatic plants such as seaweed in the unsteady flow fields generated by free-surface waves, we investigate a novel device based on piezoelectric plates to harvest energy from oscillatory cross flows. Towards this end, numerical studies are conducted using a flow-structure-electric interaction model to understand the underlying physical mechanisms involved in the dynamics and energy harvesting performance of one or a pair of piezoelectric plates in an oscillatory cross flow. In a single-plate configuration, both periodic and irregular responses have been observed depending on parameters such as normalized plate stiffness and Keulegan-Carpenter number. Large power harvesting is achieved with the excitation of natural modes. Besides, when the time scale of the motion and the intrinsic time scale of the circuit are close to each other the power extraction is enhanced. In a two-plate configuration with tandem formation, the hydrodynamic interaction between the two plates can induce irregularity in the response. In terms of energy harvesting, two counteracting mechanisms have been identified, shielding and energy recovery. The shielding effect reduces plate motion and energy harvesting, whereas with the energy recovery effect one plate is able to recovery energy from the wake of

*Corresponding author. Email: qizhu@ucsd.edu

another for performance enhancement. The competition between these mechanisms leads to constructive or destructive interactions between the two plates. These results suggest that for better performance the system should be excited at its natural period, which should be close to the intrinsic time scale of the circuit. Moreover, using a pair of plates in a tandem formation can further improve the energy harvesting capacity when conditions for constructive interaction are satisfied.

Keywords: piezoelectric, flexible plate, energy harvesting, oscillatory flow

1 Introduction

Traditional designs of flow energy harvesters feature localized energy extraction. For example, in both horizontal and vertical axis turbines the energy extraction occurs at the rotational axes, where generators are installed. This characteristic has been inheritted in many newly developed systems with oscillatory rather than rotational motions. These devices often contain a single or multiple rigid bodies. Although the energy transfer from the flow field to the device happens over the entire body surface, the kinetic energy of the body is transfered to electricity locally, usually at the hinges [1, 2].

Unlike systems based on rotational or oscillatory motions of rigid objects, flexible flow energy harvesters are more environmentally friendly and easily adaptable to various environments [3]. For these systems localized energy extraction is not suitable since the flow-induced deformation occurs all over the body. Instead, distributed energy extraction via materials such as piezoelectric pairs provides a more appropriate option [4, 5, 6, 7]. Early studies concentrate on the extraction of the kinetic energy

This is the accepted manuscript of the article: Zhu, Q., & Xiao, Q. (2024). Dynamics of seaweed-inspired piezoelectric plates for energy harvesting from oscillatory cross flow. Bioinspiration & Biomimetics, 19(4), Article 046004. https://doi.org/10.1088/1748-3190/ad43d1

in uniform incoming flows. For example, Allen and Smits proposed a piezoelectric membrane inspired by an eel [8]. The membrane was placed in the wake of a blunt body, where the von Kármán vortex street triggered vibrations of the membrane to generate electricity.

If properly designed, a structure itself may start oscillating in a uniform flow due to instabilities associated with flow-structure interaction. A typical example is the flow-induced flapping motion of a flag [9, 10, 11]. Based on this principle, it has been suggested that flexible plates covered with piezoelectric materials may be used for energy harvesting from flow-induced vibrations. Two different designs have been reported in the literature. The first design features a single patch of piezoelectric pair [12]. In this system the energy harvesting is related to the integrated curvature over the length of the plate. This design is suitable in scenarios when the fundamental flapping mode is excited. When higher modes are excited there could be saddle points along the plate where the curvature changes sign. This reduces the efficiency of energy harvesting since curvatures at different locations partially cancel each other. This issue can be avoided with the second design, in which there are multiple piezoelectric patches distributed along the plate so that energy is extracted from the local curvature rather than the integrated effect [13, 14].

Compared with a flag that is fixed at its leading edge, an inverted flag with its trailing edge fixed is more unstable and thus promises higher flow energy harvesting capacity [15]. The performance of an inverted piezoelectric flag has been investigated numerically by Shoele and Mittal [16]. The results indicate that large-amplitude responses and thus relatively high energy extraction can be achieved in a wide range of parameters. In terms of energy harvesting, the optimal performance occurs when

the oscillation time scale of the flag matches the intrinsic time scale of the circuit, a phenomenon also observed in a piezoelectric flag with the leading edge fixed [14, 17]. This study was later extended to the scenario of energy harvesting from an unsteady flow field which includes a steady mean flow and an oscillatory flow, although the mean flow is still the primary energy source [18]. Significant improvement in energy harvesting capacity has been observed by replacing the Resistor-Capacitor (RC) circuit used in these studies with Resistor-Inductor-Capacitor circuit [19]. In another recent investigation, the potential for flow energy harvesting by using an inclined inverted flag has been examined numerically [20]. However, in this model no piezoelectric material was included. Instead, the focus was on the conversion of the kinetic energy of the fluid to the strain energy inside the flag.

In fact, an unsteady flow field, such as the one created by free-surface waves, provides a source of energy that is easier to harvest since the unsteadiness comes from the flow itself so that no flow-induced instability (which depends heavily on the design of the system and the flow condition) is needed. This is clearly demonstrated in the motion and deformation of aquatic plants such as seaweeds excited by the time-dependent mechanical loads from ocean waves. In an unsteady flow field, an energy harvester is not only able to extract kinetic energy related to flow speed but also potential energy related to flow acceleration. Indeed, in a steady flow field, the mechanical load on an immersed structure is drag based, which is proportional to the square of the incoming flow speed. In an unsteady flow field, on the other hand, the load on the structure contains two parts, the drag-based part and the added-mass (buoyancy) part. The latter one is proportional to the acceleration. The pressure gradient associated with flow acceleration creates a potential energy field, from which

This is the accepted manuscript of the article: Zhu, Q., & Xiao, Q. (2024). Dynamics of seaweed-inspired piezoelectric plates for energy harvesting from oscillatory cross flow. Bioinspiration & Biomimetics, 19(4), Article 046004. https://doi.org/10.1088/1748-3190/ad43d1

energy harvesting may be achieved. For example, Xie et al. propose a wave energy harvesting system consisting of a sphere supported by a vertical cantilever beam [21]. The system bends under the horizontal load from the waves, which is predicted by using a simplified Morison-type approach. Patches of piezoelectric pairs are attached to the beam for energy extraction. The energy harvesting performance at different parameters related to the beam and the wave has been documented. After that, the capacity of piezoelectric seaweed to extracted energy from ocean waves has been examined numerically [22]. More recently, seaweed-like triboelectric nanogenerator has been proposed to harvest energy from ocean waves [23, 24]. Unfortunately, in these studies there is little investigation into the underlying physics, especially the fluid-structure interaction mechanisms.

In summary, most of the existing fluid-structure interaction studies about flow energy harvesters based on flexible piezoelectric plates consider steady incoming flow as the primary source of energy. In comparison with these systems, a system that harvests energy from unsteady flows is more robust and much easier to design since it does not require the strict conditions to be satisfied for flow-induced instability. To date there has been little comprehensive investigation into the underlying physics in this energy harvesting method. It is thus the purpose of this study to illustrate the flow-structure-electric interaction mechanisms involved in the dynamics and energy harvesting capacity of these plates through numerical simulations.

Towards this end we have developed a fully-coupled flow-structure-electric model based on the immersed-boundary framework. The model has been applied to simulate the dynamics and energy harvesting performance of a single piezoelectric plate or a pair of such plates in a tandem configuration. For physical cleanliness, we consider

This is the accepted manuscript of the article: Zhu, Q., & Xiao, Q. (2024). Dynamics of seaweed-inspired piezoelectric plates for energy harvesting from oscillatory cross flow. Bioinspiration & Biomimetics, 19(4), Article 046004.
https://doi.org/10.1088/1748-3190/ad43d1

an oscillatory cross flow as the background flow field. Physically, this resembles the flow field generated by shallow water waves whose wave lengthes are much larger than the length scale of the energy harvesting system itself. For better performance when higher modes are excited, the multiple patch design [14] is employed. With a high-fidelity physical depiction, we aim at illustrating the underlying mechanisms that contribute to the energy harvesting capacity, based on which design principles may be developed.

The rest of the paper is organized as follows. We start by describing the physical problem to be studied, including the structural designs of the plates and flow conditions they work in. Mathematical formulations, including governing equations of the fluid dynamics, the structural dynamics, and the piezoelectric system, will then be presented. There is also a brief description of the numerical method (details can be found in the literature). This is followed by the numerical results and discussions about the underlying fluid-structure interaction mechanisms. Finally, conclusions are drawn.

2 Problem description

As shown in Fig. 1, we consider one or two flexible plates in an oscillatory cross flow whose speed U is time dependant. One end of a plate (the bottom end) is fixed, whereas the other end (the top end) is free. The length of the plates is L. The thickness of the plate is negligibly small in comparison with its length. In the two-plate scenario, the distance between the two plates is D.

Along its length, the plate contains pairs of piezoelectric patches that follow the

This is the accepted manuscript of the article: Zhu, Q., & Xiao, Q. (2024). Dynamics of seaweed-inspired piezoelectric plates for energy harvesting from oscillatory cross flow. Bioinspiration & Biomimetics, 19(4), Article 046004.
https://doi.org/10.1088/1748-3190/ad43d1

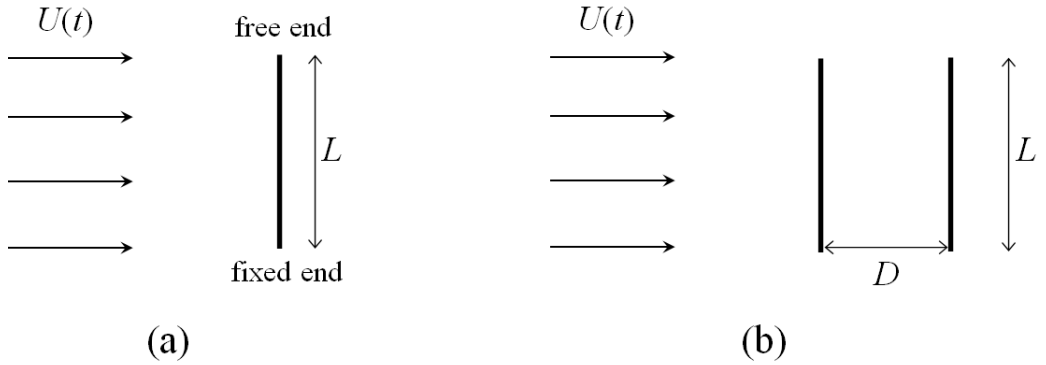

Figure 1: (a) A single flexible plate and (b) a pair of tandem plates in cross flows with time-varying speed.

local deformation of the plate [14]. As a patch pair is bent, it is stretched on one side and compressed on the other so that electric voltage between the positive electrodes is generated. For energy harvesting, these positive electrodes are connected with a purely resistive circuit, in which the voltage induces an electric current. Meanwhile, the electric voltage on the patch also creates an internal torque on the plate so that the mechanical and electric processes are coupled. In the limiting case when these patches are infinitesimally small, they can be viewed as continuously distributed on the plate and the voltage they generate is continuous along the length of the plate.

The time variation of the flow speed U is assumed to be sinusoidal so that $U(t) = U_0 \sin(\omega t)$. This velocity profile is consistent with the velocity caused by a shallow-water wave except that the wave also generates flow in the vertical direction. This vertical component is usually much weaker than the horizontal one, especially in the vicinity of the bottom. It is thus not considered in our model.

The computational domain and the boundary conditions are shown in Fig. 2.

This is the accepted manuscript of the article: Zhu, Q., & Xiao, Q. (2024). Dynamics of seaweed-inspired piezoelectric plates for energy harvesting from oscillatory cross flow. Bioinspiration & Biomimetics, 19(4), Article 046004.
https://doi.org/10.1088/1748-3190/ad43d1

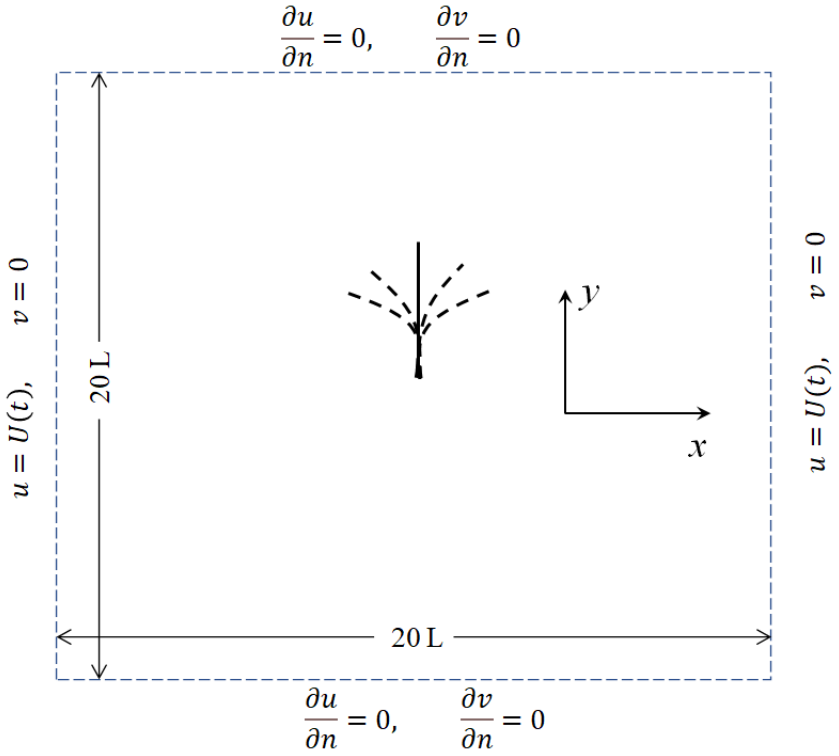

Figure 2: The computational domain and the boundary conditions. The normal direction n points out of the domain.

This is the accepted manuscript of the article: Zhu, Q., & Xiao, Q. (2024). Dynamics of seaweed-inspired piezoelectric plates for energy harvesting from oscillatory cross flow. Bioinspiration & Biomimetics, 19(4), Article 046004.
https://doi.org/10.1088/1748-3190/ad43d1

3 Materials and methods

3.1 Governing equations

Under the immersed-boundary frame work, the governing equations for the fluid dynamics are

$$\rho\left(\frac{\partial \mathbf{u}}{\partial t}+\mathbf{u}\cdot\nabla\mathbf{u}\right)=-\nabla p+\mu\nabla^2\mathbf{u}+\mathbf{f}(\mathbf{x},t), \tag{1}$$

and

$$\nabla\cdot\boldsymbol{u}=0, \tag{2}$$

where $\mathbf{x}\equiv(x,y)$ stands for the Eulerian coordinate shown in Fig. 2. $\mathbf{u}\equiv(u,v)$ is the flow velocity. ρ and μ are the density and dynamic viscosity of the fluid, respectively. p is the pressure. $\mathbf{f}$ is body force density exerted by the immersed structure on the fluid.

The structural equation is given as

$$m\frac{\partial^2\mathbf{X}}{\partial t^2}=\frac{\partial}{\partial s}\left(\sigma\boldsymbol{\tau}\right)-\frac{\partial^2}{\partial s^2}\left(k_b\frac{\partial^2\mathbf{X}}{\partial s^2}\right)+\frac{\partial}{\partial s}\left(\mathcal{A}\frac{\partial\mathcal{V}}{\partial s}\mathbf{n}\right)-\mathbf{F}, \tag{3}$$

where m is the mass per unit length of the plate. $\mathbf{X}$ is the instantaneous location of the plate. s is a Lagrangian coordinate along the body. $\boldsymbol{\tau}$ and $\mathbf{n}$ are the unit tangential and normal vectors of the body, respectively. $\mathcal{V}$ is the voltage in the circuit. $\mathcal{A}$ is the coupling coefficient, which is determined by the material properties of the piezoelectric patches. $\mathbf{F}$ is the force density applied by the the surrounding fluid to the structure. σ is the tension inside the plate, which is employed as a Lagrangian multiplier to restrict the local stretching so that the inextensibility constraint is satisfied, i.e. $(\partial\mathbf{X}/\partial s)\cdot(\partial\mathbf{X}/\partial s)=1$.

This is the accepted manuscript of the article: Zhu, Q., & Xiao, Q. (2024). Dynamics of seaweed-inspired piezoelectric plates for energy harvesting from oscillatory cross flow. Bioinspiration & Biomimetics, 19(4), Article 046004. https://doi.org/10.1088/1748-3190/ad43d1

The governing equation of the circuit is

$$C\frac{\partial \mathcal{V}}{\partial t} = -\frac{1}{R}\mathcal{V} - \mathcal{A}\frac{\partial}{\partial t}\left(\frac{\partial^2 \mathbf{X}}{\partial s^2}\cdot \mathbf{n}\right), \tag{4}$$

where C is the linear capacitance of the piezoelectric element. R is the resistance in the circuit.

Equations (1) to (4) form a fully-coupled mathematical formulation for the fluid-structure-electric interaction problem involved in the flow energy harvester defined in §2.

The harvested power P is

$$P = \frac{1}{R}\int_0^L \mathcal{V}^2 ds. \tag{5}$$

The problem is normalized by using L, T, ρL^2, and $LT^{-1}\sqrt{\rho L/C}$ as the characteristic length, time, mass per unit length, and voltage, respectively. The dimensionless forms of Eqns. (3) and (4) are

$$m\frac{\partial^2 \mathbf{X}}{\partial t^2} = \frac{\partial}{\partial s}(\sigma \boldsymbol{\tau}) - \frac{\partial^2}{\partial s^2}\left(\kappa\frac{\partial^2 \mathbf{X}}{\partial s^2}\right) + \frac{\partial}{\partial s}\left(\alpha\sqrt{\kappa}\frac{\partial \mathcal{V}}{\partial s}\mathbf{n}\right) - \mathbf{F}, \tag{6}$$

and

$$\beta\frac{\partial \mathcal{V}}{\partial t} = -\mathcal{V} - \alpha\beta\sqrt{\kappa}\frac{\partial}{\partial t}\left(\frac{\partial^2 \mathbf{X}}{\partial s^2}\cdot \mathbf{n}\right), \tag{7}$$

where $\alpha = \mathcal{A}/\sqrt{k_b C}$, $\beta = CR/T$, and $\kappa = k_b/(\rho L^5 T^{-2})$. The normalized power extraction is

$$P = \frac{1}{\beta}\int_0^1 \mathcal{V}^2 ds. \tag{8}$$

For convenience, in Eqns. (6) to (8) we use the same symbols (s, t, m, $\mathbf{X}$, σ, $\mathbf{F}$, $\mathcal{V}$, and P) to represent the dimensionless forms of the corresponding variables in Eqns.

This is the accepted manuscript of the article: Zhu, Q., & Xiao, Q. (2024). Dynamics of seaweed-inspired piezoelectric plates for energy harvesting from oscillatory cross flow. Bioinspiration & Biomimetics, 19(4), Article 046004.
https://doi.org/10.1088/1748-3190/ad43d1

(3) to (5).

3.2 Immersed-boundary formulation and numerical implementation

The coupled fluid-structure-electric equations in §3.1 are solved by using a model we have developed and validated in previous publications [19, 26] based on an immersed-boundary framework in the literature [25, 27]. Specifically, the force density on the fluid exerted by the stricture $\mathbf{f}$ and the force density on the structure exerted by the fluid $\mathbf{F}$ are related through a Dirac Delta function so that

$$\mathbf{f}(\mathbf{x},t) = \int_{\Gamma} \mathbf{F}(s,t)\delta(\mathbf{X}(s,t)-\mathbf{x})ds, \tag{9}$$

where Γ represents the structure. Furthermore, to enforce the no-flux and no-slip conditions at the fluid-structure interface, the force $\mathbf{F}$ is evaluated by using a penalty method [25, 26]

$$\mathbf{F}(s,t) = \alpha_n \int_0^t \left[\mathbf{U}(s,\tau)-\mathbf{V}(s,\tau)\right] d\tau + \beta_n \left[\mathbf{U}(s,t)-\mathbf{V}(s,t)\right], \tag{10}$$

where $\mathbf{V}$ is the structural velocity and $\mathbf{U}$ is the fluid velocity at the fluid-structure interface obtained as

$$\mathbf{U}(s,t) = \int_{\Omega} \mathbf{u}(\mathbf{x},t)\delta(\mathbf{x}-\mathbf{X}(s,t))d\mathbf{x}, \tag{11}$$

where Ω is the fluid domain. α_n and β_n are numerical parameters with sufficiently large negative values.

Thus formulated, the equations, including the fluid dynamics equations, the structural dynamics equation, and the circuit equation, are solved with a finite-difference

This is the accepted manuscript of the article: Zhu, Q., & Xiao, Q. (2024). Dynamics of seaweed-inspired piezoelectric plates for energy harvesting from oscillatory cross flow. Bioinspiration & Biomimetics, 19(4), Article 046004. https://doi.org/10.1088/1748-3190/ad43d1

approach, including a second-order spatial discretization method and a Crank-Nicholson time integration method. An iteration algorithm is employed for the fluid-structure-circuit coupling. Details of this method and validations can be found in previous publications [27, 26, 28, 16].

4 Results

4.1 A single plate

We start by considering a single plate as shown in Fig. 1a. In the normalized form, the fluid density ρ, the length of the plate L, and the period of the oscillatory flow T are all set to be unity. Following previous studies [14, 16, 18], we choose $\alpha = 0.3$. This value of α is typical for piezoelectric materials such as lead zirconate titanate [16]. Unless otherwise specified, the circuit property β is chosen to be 0.5. The mass per unity length of the plate is chosen to be 0.5. The dynamics of the system are thus determined by the following factors:

- The stiffness κ, which determines the natural frequencies of the plate;
- The Reynolds number R_e, defined as $\rho L U_0/\mu$;
- The Keulegan-Carpenter number K_C, defined as $U_0 T/L$, which measures the ratio between the 'stroke' of fluid particle (i.e., the distance a fluid particle travels before it changes direction) and the length of the plate. This parameter depends on both the strength and unsteadiness of the flow field.

In the following simulations, the ranges of the parameters we consider are $\kappa \in [10^{-3}, 4.5]$ and $K_C \in [0.5, 2]$. Considering the capacity of the immersed-boundary

This is the accepted manuscript of the article: Zhu, Q., & Xiao, Q. (2024). Dynamics of seaweed-inspired piezoelectric plates for energy harvesting from oscillatory cross flow. Bioinspiration & Biomimetics, 19(4), Article 046004.
https://doi.org/10.1088/1748-3190/ad43d1

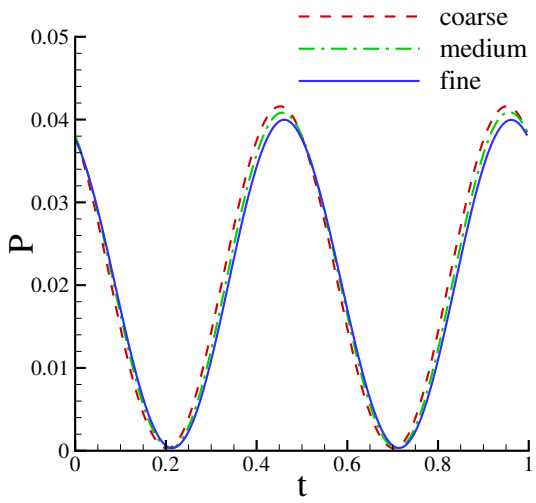

Figure 3: Sensitivity of the predicted power extraction P with different computational meshes. $K_C = 1.0$, $\kappa = 1.0$. The results are extracted from the 9th period (for convenience, the starting time in the time history is shifted to 0). $\Delta t = 10^{-4}$.

model used here, the Reynolds number is fixed at 100, which is achieved by setting $\mu \propto U_0$ so that the value of R_e is not affected by the variation of U_0. For example, at $K_C = 0.5$ we have $U_0 = 0.5$ and $\mu = 0.005$, whereas at $K_C = 1.0$ we use $U_0 = 1.0$ and $\mu = 0.01$ to keep the Reynolds number unchanged.

Sensitivity tests have been conducted to corroborate the accuracy of the numerical model and determine the numerical parameters. Figure 3 demonstrates time histories of P obtained with three meshes, a coarse one in which near the body $\Delta x = \Delta y = 0.033$ with 39 uniformly distributed grids on the plate (Δx and Δy are the sizes of the fluidic grids in x and y directions, respectively), a medium one in which $\Delta x = \Delta y = 0.025$ with 53 grids on the plate, and a fine one in which $\Delta x = \Delta y = 0.0167$ with 78 grids on the plate. It is seen that P is relatively insensitive to the mesh. The time-averaged values of P in these three cases are 0.0209, 0.0205, and 0.0202,

This is the accepted manuscript of the article: Zhu, Q., & Xiao, Q. (2024). Dynamics of seaweed-inspired piezoelectric plates for energy harvesting from oscillatory cross flow. Bioinspiration & Biomimetics, 19(4), Article 046004.
https://doi.org/10.1088/1748-3190/ad43d1

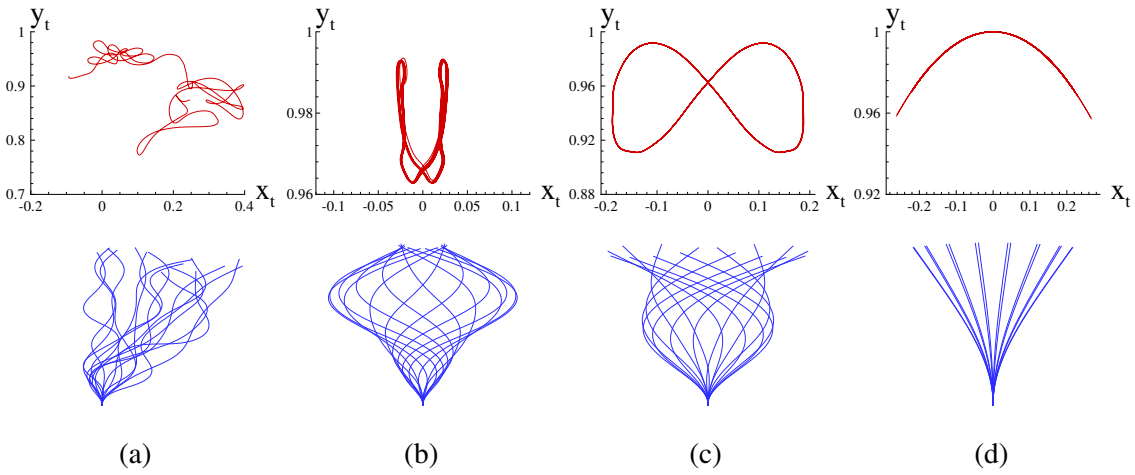

Figure 4: (Upper) Trajectories of the top end (x_t, y_t) and (Lower) snapshots of the body deformation for (a) irregular response when $\kappa = 10^{-3}$, (b) response dominated by the third natural mode when $\kappa = 0.02$, (c) response dominated by the second natural mode when $\kappa = 0.1$, and (d) response dominated by the first natural mode when $\kappa = 2.0$. $K_C = 0.5$.

respectively. Sensitivity of the results with respect to the time step Δt has also been tested with Δt varying from 2.5×10^{-5} to 1.5×10^{-4}. Within this range of Δt the time histories of P are graphically indistinguishable from each other so that they are not shown. Additional sizes of the computational domain, 30×30 and 40×40, have also been tested. The effect on the results is also negligibly small. Based on these tests, hereafter we choose the fine mesh with $\Delta t = 2.5 \times 10^{-5}$ and a 20×20 computational domain (the one shown in Fig. 2).

Two distinctive structural responses have been observed, non-periodic irregular response (Fig. 4a) and periodic response (Figs. 4b, c and d). In the periodic response the plate undergoes cyclic deformation whose period coincides with that of the external flow. The deformation is usually dominated by a natural mode of the plate. Within the range of parameters considered in this study, the 1st (Fig. 4d), 2nd (Fig. 4c), and 3rd (Fig. 4b) natural modes can be excited as the stiffness

This is the accepted manuscript of the article: Zhu, Q., & Xiao, Q. (2024). Dynamics of seaweed-inspired piezoelectric plates for energy harvesting from oscillatory cross flow. Bioinspiration & Biomimetics, 19(4), Article 046004.
https://doi.org/10.1088/1748-3190/ad43d1

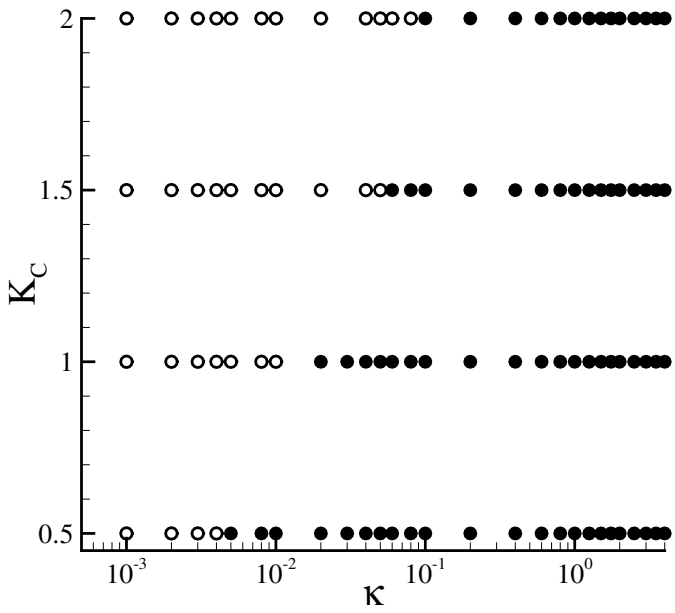

Figure 5: Occurrence of irregular (○) and periodic (●) responses at various combinations of κ and K_C.

κ is reduced. Further reduction of κ leads to irregular response so that no higher modes have been observed. For structural safety and reliable energy harvesting, the irregular response shall be avoided since it is unpredictable.

Figure 5 demonstrates a map of periodic versus irregular responses at different combinations of κ and K_C. It is seen that at a given K_C, the response becomes irregular when κ falls below a threshold value. This value increases when K_C is raised. For example, when $K_C = 0.5$, the transition to irregularity occurs at $\kappa = 5 \times 10^{-3}$. When K_C is raised to 1, the threshold value of κ becomes 2×10^{-2}. At the upper end of K_C considered in this study (i.e., $K_C = 2$), this value rises to 0.1.

In periodic responses, we characterize the motion and energy harvesting perfor-

This is the accepted manuscript of the article: Zhu, Q., & Xiao, Q. (2024). Dynamics of seaweed-inspired piezoelectric plates for energy harvesting from oscillatory cross flow. Bioinspiration & Biomimetics, 19(4), Article 046004.
https://doi.org/10.1088/1748-3190/ad43d1

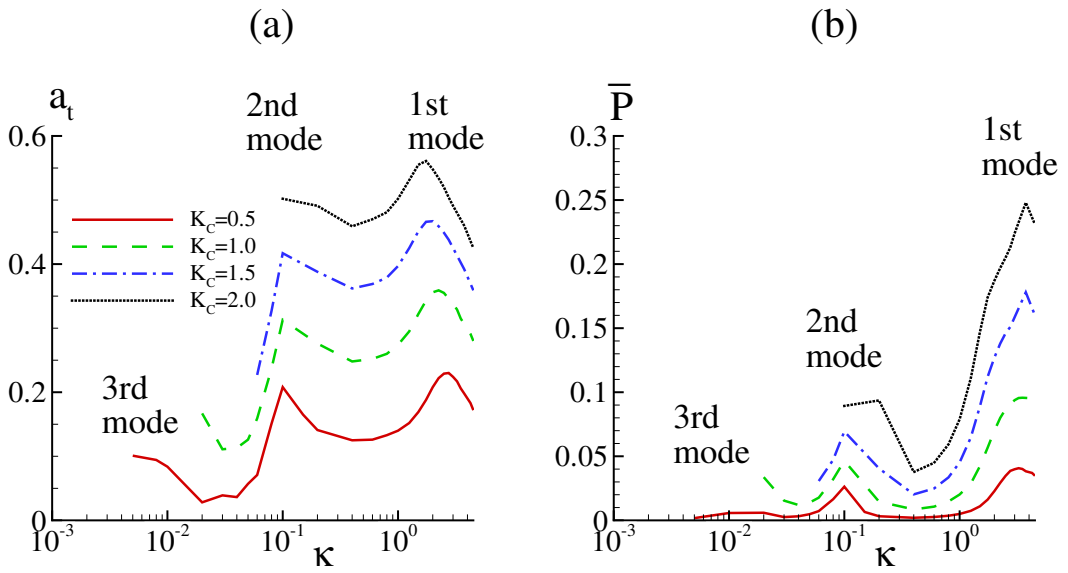

Figure 6: (a) Amplitude of the top end a_t and (b) time-averaged power extraction capacity $\overline{P}$ as functions of κ at various values of K_C. The modes in this figure are illustrated in Fig. 4.

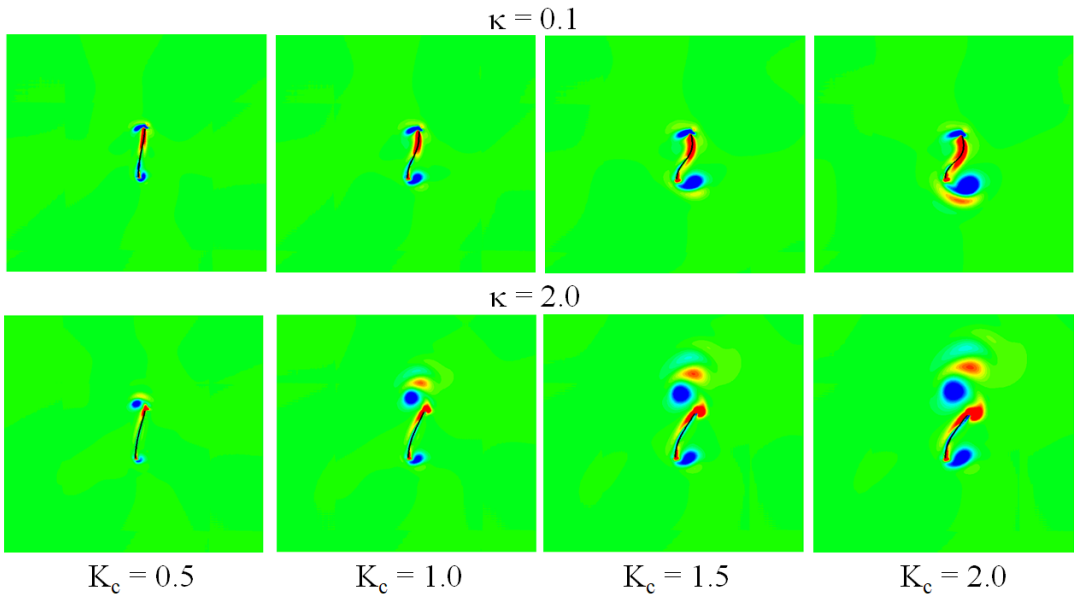

Figure 7: Flow fields visualized through vorticity contour ranging from -10 (blue) and 10 (red) at $\kappa = 0.1$ and 2.0 with various values of K_C for a single plate. $t = T/2$.

This is the accepted manuscript of the article: Zhu, Q., & Xiao, Q. (2024). Dynamics of seaweed-inspired piezoelectric plates for energy harvesting from oscillatory cross flow. Bioinspiration & Biomimetics, 19(4), Article 046004. https://doi.org/10.1088/1748-3190/ad43d1

mance of the system using two parameters, the amplitude of the motion of the top end in the horizontal direction a_t, and the time-averaged power extraction $\overline{P}$ (i.e., the value of P defined in Eq. (8) averaged over one flow cycle after the periodic response is established). The dependencies of these two quantities upon κ and K_C are shown in Fig. 6. It is seen that in general higher values of K_C leads to larger motion and more energy harvested. This is expected since the increase in K_C is achieved by raising U_0, and subsequently, higher kinetic and potential energy in the surrounding flow field. Excitations of the first three natural modes of the plate create peaks in the a_t and $\overline{P}$ vs. κ curves when K_C is fixed. In terms of $\overline{P}$, higher peaks occur when κ increases. This is explained by that fact that with $\alpha = \mathcal{A}/\sqrt{k_b C}$ fixed at 0.3, when the capacitance does not change, the coupling coefficient $\mathcal{A}$ has to increase with κ. This is shown more clearly in the dimensionless circuit equation (Eq. (7)), where κ is present in the last term so that its value directly affects the power extraction.

We concentrate on two representative values of κ, 0.1 and 2.0, referred to as the *soft plate* and the *stiff plate*, respectively. In these two cases periodic response has been found within the whole range of K_C we consider. In the soft plate case the dominant deformation mode is the 2nd mode, whereas in the stiff plate case the dominant mode is the 1st mode.

We plot the near-body flow field around the stiff and the soft plates in Fig. 7. For convenience, in this figure and the other snapshots of the flow field we shift the time so that $t = 0$ corresponds to the start of the flow cycle after periodic response is established. In both the stiff and the soft plate cases the Keulegan-Carpenter number has similar effect - when this dimensionless number is increased, more pronounced vortex shedding from the body is observed. On the other hand, in terms of the

This is the accepted manuscript of the article: Zhu, Q., & Xiao, Q. (2024). Dynamics of seaweed-inspired piezoelectric plates for energy harvesting from oscillatory cross flow. Bioinspiration & Biomimetics, 19(4), Article 046004.
https://doi.org/10.1088/1748-3190/ad43d1

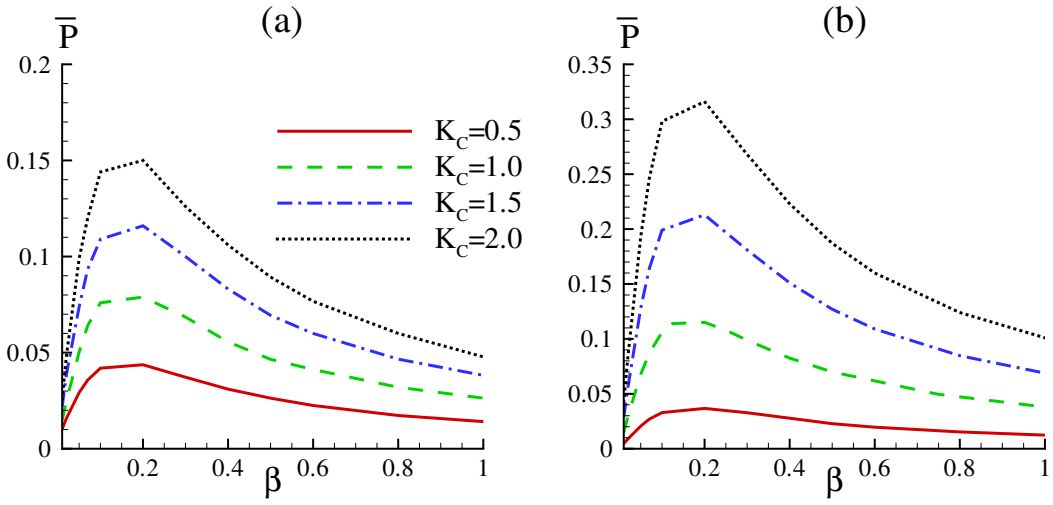

Figure 8: Time-averaged power extraction capacity $\overline{P}$ as function of β at various values of K_C when (a) $\kappa = 0.1$ and (b) $\kappa = 2.0$.

detailed vorticity distribution there exist considerable differences between the two plates. Most notably, with the stiff plate there are strong vortices shed from the top end. However, in the soft plate the vortex shedding from the top end is greatly mitigated. This is attributed to the diminished relative motion between the free end of the plate and the surrounding flow (i.e., the feathering effect) when the stiffness is low. This phenomenon will have interesting effects on the hydrodynamic interaction between two tandem plates, which will be discussed later.

To examine the effect of the electric parameters, we simulate the soft and stiff plates with β (which combines the resistance R and the capacitance C) ranging from 0.01 to 1. According to the results (see Fig. 8), optimal power harvesting is achieved when $\beta \sim 0.2$. This is reminiscent of the finding that when the time scale of structural deformation matches the intrinsic time scale of the circuit, the power extraction is maximized [14, 16]. In the literature, this occurs when $\beta\omega = O(1)$ (ω is

This is the accepted manuscript of the article: Zhu, Q., & Xiao, Q. (2024). Dynamics of seaweed-inspired piezoelectric plates for energy harvesting from oscillatory cross flow. Bioinspiration & Biomimetics, 19(4), Article 046004. https://doi.org/10.1088/1748-3190/ad43d1

the vibrating frequency of the structure) [16]. It is necessary to point out there are differences in terms of normalization and the definition of β between their study and ours. In our model the parameter corresponding to $\beta\omega$ is $2\pi\beta$, whose value at optimal performance is around 1.2 according to the results shown in Fig. 8. Therefore, our prediction about the effect of β is consistent with previous reports.

The effect of β on the structural deformation is relatively small. In all the cases we study, within the range of β the variation in a_t is lower than 5%. The implication is that with a purely resistive circuit we consider, the structure-electric coupling is mostly one-directional (i.e., from the structure to the electric system). In this scenario, it is possible to design the structural and the electric systems independently. On the other hand, if an inductive-resistive circuit is used [29, 17, 30], the coupling effect might be much stronger so that the systems have to be designed together for optimization.

4.2 Two tandem plates

In this part we study the dynamics and energy harvesting performance of two tandem plates (see Fig. 1b). For simplicity we assume that the two plates have the same stiffness. Two values of κ, 0.1 and 2.0, are considered. To characterize the effect of hydrodynamic interactions between the plates, we defined two parameters, the amplitude amplification factor A_a and the power amplification factor A_P. Here $A_a = (a_{t1} + a_{t2}) / (2a_t)$, where a_{t1} and a_{t2} are the horizontal amplitudes of the top ends of the two plates in formation, and a_t is the corresponding value of a stand-alone plate with the same plate stiffness κ and Keulegan-Carpenter number K_C discussed in §4.1. Similarly, $A_P = \left(\overline{P}_1 + \overline{P}_2\right) / \left(2\overline{P}\right)$, where $\overline{P}_1$ and $\overline{P}_2$ are the mean power

This is the accepted manuscript of the article: Zhu, Q., & Xiao, Q. (2024). Dynamics of seaweed-inspired piezoelectric plates for energy harvesting from oscillatory cross flow. Bioinspiration & Biomimetics, 19(4), Article 046004.
https://doi.org/10.1088/1748-3190/ad43d1

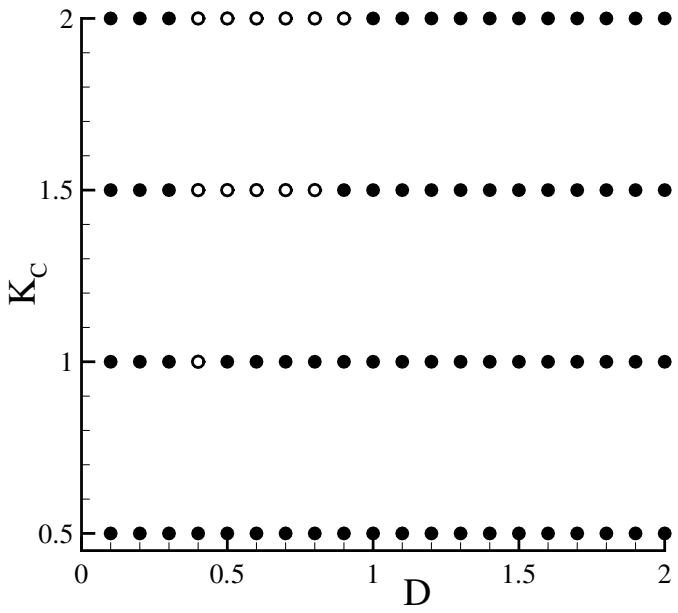

Figure 9: Occurrence of irregular (○) and periodic (●) responses with two plates at various combinations of D and K_C. $\kappa = 0.1$.

extraction of the two plates in formation, and $\overline{P}$ is the mean power extraction of a single plate under the same conditions.

The interaction between the two plates may change the nature of the response. For example, when $\kappa = 0.1$ the response of a single plate remains periodic within the whole range of K_C we consider (see Fig. 5). However, in the two-plate configuration it has been discovered that with the same κ the response may become irregular at certain ranges of separation D. As shown in Fig. 9, there is no irregular case when $K_C = 0.5$. When K_C is increased to 1.0, irregular response occurs when D is around 0.4. The range of D that leads to irregularity increases with higher K_C. For example, if $K_C = 1.5$ this range is (0.4,0.8). It becomes (0.4,0.9) when $K_C = 2.0$.

This is the accepted manuscript of the article: Zhu, Q., & Xiao, Q. (2024). Dynamics of seaweed-inspired piezoelectric plates for energy harvesting from oscillatory cross flow. Bioinspiration & Biomimetics, 19(4), Article 046004. https://doi.org/10.1088/1748-3190/ad43d1

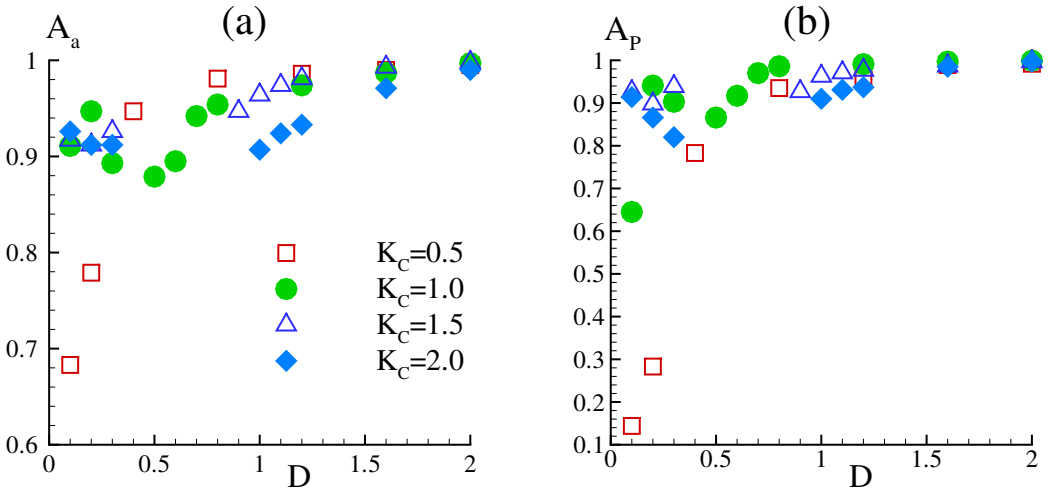

Figure 10: Amplification factors A_a (a) and A_P (b) for two plates at various combinations of D and K_C. $\kappa = 0.1$.

In the periodic response, the amplification factors A_a and A_P for the soft-plate case at different combinations of D and K_C are displayed in Fig. 10. In all the cases shown in that figure, both A_a and A_P remain smaller than one. This suggests that at this κ the shielding effect from the neighboring plate always reduce the motion and the energy harvesting capacity. The effect is particularly pronounced when both K_C and D are small. For example, when $K_C = 0.5$ and $D = 0.1$, $A_a = 0.68$ and A_P is as small as 0.14. This is explained by the fact that when K_C is small, the bending deformation of the plates is also small so that the shielding effect is strong.

The stiff plate case (i.e., $\kappa = 2.0$) displays completely different behavior. First, there is no irregular response within the range of D and K_C considered in this study. Another notable phenomenon is that when K_C is below 1.5, there exist ranges of D in which the amplification factors A_a and A_P are actually larger than one (see Fig. 11), i.e., the hydrodynamic interactions between the two plates enhance the motion

This is the accepted manuscript of the article: Zhu, Q., & Xiao, Q. (2024). Dynamics of seaweed-inspired piezoelectric plates for energy harvesting from oscillatory cross flow. Bioinspiration & Biomimetics, 19(4), Article 046004.
https://doi.org/10.1088/1748-3190/ad43d1

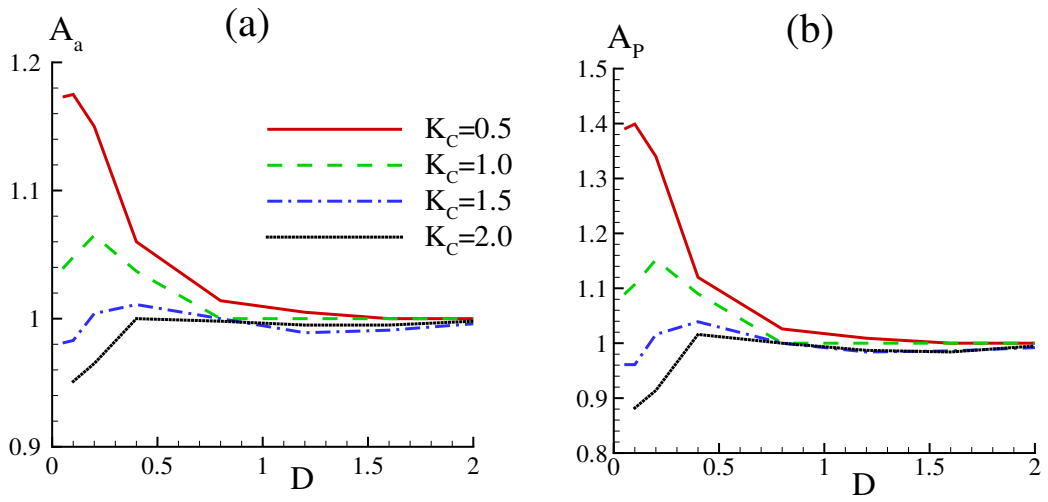

Figure 11: Amplification factors A_a (a) and A_P (b) for two plates at various combinations of D and K_C. $\kappa = 2.0$.

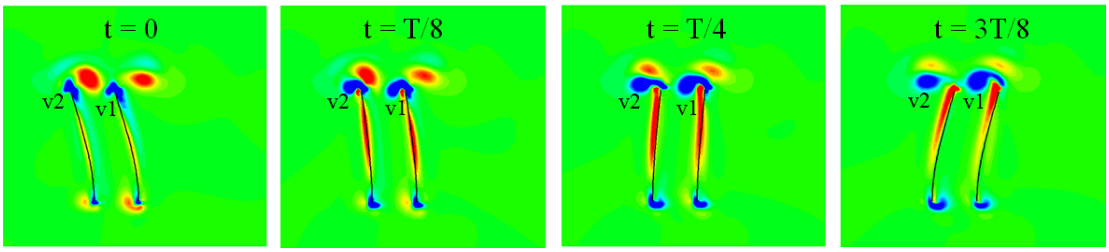

Figure 12: Flow fields visualized through vorticity contour ranging from -10 (blue) and 10 (red) for two plates during half the flow cycle. $\kappa = 2.0$, $K_C = 0.5$ and $D = 0.4$.

and energy harvesting capacity of the individual plates. The largest enhancement occurs when $K_C = 0.5$ and $D = 0.1$, where an 18% increase in the motion amplitude and a 40% increase in power extraction are recorded.

This constructive interaction between neighboring plates is explained by the detailed vorticity field around the structures, especially the vortices that shed from the top ends of the plates. To illustrate this mechanism, in Fig. 12 we plot the motions of the two plates and evolution of the near-body vorticity field during the first half

This is the accepted manuscript of the article: Zhu, Q., & Xiao, Q. (2024). Dynamics of seaweed-inspired piezoelectric plates for energy harvesting from oscillatory cross flow. Bioinspiration & Biomimetics, 19(4), Article 046004. https://doi.org/10.1088/1748-3190/ad43d1

of a flow period when $K_C = 0.5$ and $D = 0.4$. A notable feature in this figure is the strong vortex (marked as 'v1' in the figure) shed from the top end of the plate on the right (referred to as plate 1). This vortex is trapped in the gap between the two plates. The low pressure it creates induce a force near the top end of the plate on the left (plate 2). This additional force is in the same direction of the plate motion so that it pumps mechanical energy into plate 2. In this sense, plate 2 is able to harvest energy from the wake of plate 1 so that its motion, and subsequently, power extraction, are increased. Similarly, during the second half of the period plate 1 can harvest energy from the wake of plate 2 for performance enhancement.

This mechanism only works within a relatively narrow region of parameters. For example, when D is too large, vortex v1 will be too far from plate 2 to have any effect on it. On the other hand, when D is too small and/or K_C is too large, the vortex v1 will merge with its counterpart shed from plate 2 (marked as 'v2' in Fig. 12) and the two will shed together to the left side of plate 2. In this scenario the performance enhancement mechanism will be weakened. Moreover, when the stiffness κ is small, vortex shedding from the top ends of the plates is weak (see Fig. 7). The performance enhancement mechanism attributed to the top-end vortex shedding will be overwhelmed by the diminution mechanism due to the shielding effect discussed earlier so that no improvement in motion amplitude and power extraction is possible (see Fig. 10). The Keulegan-Carpenter number K_C also plays a role. Qualitatively, this number can be viewed as the duration of the flow in one direction before it is reversed. If it is too large, the vortices shed from the top ends of the plate will only stay in the gap for a small portion of the period before they are washed away so that the wake energy harvesting mechanism discussed in the previous paragraph will be

This is the accepted manuscript of the article: Zhu, Q., & Xiao, Q. (2024). Dynamics of seaweed-inspired piezoelectric plates for energy harvesting from oscillatory cross flow. Bioinspiration & Biomimetics, 19(4), Article 046004. https://doi.org/10.1088/1748-3190/ad43d1

too weak to achieve constructive interactions.

5 Conclusions

To understand the physical mechanisms that govern the dynamics and energy harvesting capacity of a novel device containing one or two piezoelectric plates in an oscillatory cross flow, we numerically investigate the fluid-structure-electric problem involved in this problem by using an immersed-boundary model coupled with a model of a purely resistive circuit. In our model, the piezoelectric patches are continuously distributed on the surface of the plates so that local curvature can be transformed into electric charge, which is converted into electric power through a purely resistive circuit.

We consider a dimensionless problem normalized by the fluid density, the plate length, and the period of the oscillatory flow. With the Reynolds number and the mass per unit length of the plate fixed, in the single-plate configuration the dynamic response is determined by the stiffness κ of the plate and the Keulegan-Carpenter number K_C. When $K_C = 0.5$, periodic responses dominated by the 1st, the 2nd, and the 3rd natural modes have been observed when κ is reduced. The excitation of these natural modes causes peaks in both the plate deformation and the power extraction. When κ is below a threshold value the response becomes irregular. This threshold value of κ increases with higher values of K_C.

Effects of the electric parameters, i.e., the resistance and capacitance, have also been examined. The results show that they have little effect on structural deformation but significant effect on the power extraction. Specifically, maximum power

This is the accepted manuscript of the article: Zhu, Q., & Xiao, Q. (2024). Dynamics of seaweed-inspired piezoelectric plates for energy harvesting from oscillatory cross flow. Bioinspiration & Biomimetics, 19(4), Article 046004. https://doi.org/10.1088/1748-3190/ad43d1

extraction is achieved when the intrinsic time scale of the circuit matches the time scale of structural deformation. This conclusion is consistent with findings in previous studies.

With two identical plates in a tandem formation, the dynamics and energy extraction performance depend not only on the properties of the plates themselves, but also on the distance between them. For soft plates, when this distance is within certain range the hydrodynamic interaction between the plates can induce irregular motions. In other cases, two counteracting mechanisms have been identified: (a) the shielding effect, which reduces motion and energy harvesting; (b) the energy recovery effect, in which one plate recovers energy from the wake of another to enhance motion and energy harvesting. The relative importance of these two mechanisms depends on many factors, including the stiffness of the plates, the Keulegan-Carpenter number, and the distance between plates.

According to our results, for optimal energy harvesting a plate should be designed so that its first natural frequency coincides with the frequency of the flow. Furthermore, the intrinsic time scale of the circuit should match that of the flow as well. If multiple plates in tandem formation are used, the distance between neighboring plates should be carefully chosen for constructive rather than destructive interaction.

It will be interesting to have a look at the predicted capacity of this system in dimensional form. For example, let us consider a typical case with a single plate in which $L = 10^{-2}$m, $U_0 = 10^{-2}$m/s, $T = 1$s, $\rho = 10^3$kg/m^3, $\mu = 10^{-3}$Pa s, $\kappa = 2$, $\alpha = 0.3$, and $\beta = 0.2$. According to the numerical results the dimensionless mean power output is around 0.12, corresponding to a dimensional power output of 1.2 μW if the width of the plate is 1m. The value is tiny since this is a small scale model

This is the accepted manuscript of the article: Zhu, Q., & Xiao, Q. (2024). Dynamics of seaweed-inspired piezoelectric plates for energy harvesting from oscillatory cross flow. Bioinspiration & Biomimetics, 19(4), Article 046004. https://doi.org/10.1088/1748-3190/ad43d1

to keep the Reynolds number at 100. Without considering the effect of the Reynolds number, if other dimensionless parameters and the width of the plate are fixed the power output is proportional to L^4. However, Reynolds number is expected to be an important parameter. For example, if the Reynolds number is higher, there will be less damping so that it is easier for the response to become irregular. Moreover, since Reynolds number affects the dissipation rate of vortices, it may affect the interaction between plates in an array. Clearly, investigation of the performance of the system at higher Reynolds numbers is needed.

Moreover, more comprehensive investigations are necessary to map the dynamics and performance of the system in a broader parametric space. Simulations in a broader range of plate stiffness and Keulegan-Carpenter number will be necessary to understand the exact conditions for constructive interaction to occur. In plates with finite aspect ratio, there are vortices shed from the sides in addition to the top and bottom ends. Three-dimensional effects need to be taken into account. These simulations are being conducted and the results will be reported in future publications. Besides, in the current study we have only considered two plates in the formation. It will be interesting to study cases with multiple plates and examine the possibility of constructive interaction. Also, in the current study the background flow condition is idealized – it roughly corresponds to the scenario of a flow generated by a shallow-water wave whose wavelength is much larger than the length scale of the device. Simulations with more realistic flow conditions are necessary. Finally, experimental investigations are needed to corroborate the numerical predictions in this work, and to pave the way for the development and installation of these novel energy harvesters in applications.

Data Availability Statement

The data that support the findings of this study are available from the corresponding author upon reasonable request.

References

[1] E. Renzi, A. Abdolali, G. Bellotti, and F. Dias, "Wave-power absorption from a finite array of oscillating wave surge converters," *Renewable Energy*, vol. 63, pp. 55–68, 2014.

[2] B. Drew, A. Plummer, and M. Sahinkaya, "A review of wave energy converter technology," *Proc. IMechE. Part A: J. Power and Energy*, vol. 223, pp. 887–901, 2016.

[3] C. Wang, F. Tang, and X. Zhang, "Fluid-structure interaction of bio-inspired flexible slender structures: a review of selected topics," *Bioinspir. Biomim.*, vol. 17, p. 041002, 2022.

[4] H. Akaydin, N. Elvin, and Y. Andreopoulos, "Energy harvesting from highly unsteady fluid flows using piezoelectric materials," *J. Intell. Mater. Sys. Struc.*, vol. 21, pp. 1263–1278, 2010.

[5] D. Wang and H. Ko, "Piezoelectric energy harvesting from flow-induced vibration," *J. Micromech. Microengng.*, vol. 20, p. 025019, 2010.

[6] M. Safaei, H. Sodano, and S. Anton, "A review of energy harvesting using piezoelectric materials: state-of-the-art a decade later (2008-2018)," *Smart Mater. Struct.*, vol. 20, p. 113001, 2019.

[7] B. Zhang, H. Liu, S. Zhou, and J. Gao, "A review of nonlinear piezoelectric energy harvesting interface circuits in discrete components," *Applied Mathematics and Mechanics*, vol. 43, no. 7, pp. 1001–1026, 2022.

[8] J. Allen and A. Smits, "Energy harvesting eel," *J. Fluids Struc.*, vol. 15, pp. 629–640, 2001.

[9] B. Connell and D. Yue, "Flapping dynamics of a flag in uniform stream," *J. Fluid Mech.*, vol. 581, pp. 33–67, 2007.

[10] S. Alben and M. Shelley, "Flapping states of a flag in an inviscid fluid: bistability and the transition to chaos," *Phys. Rev. Lett.*, vol. 100, p. 074301, 2008.

[11] S. Banerjee, B. Connell, and D. Yue, "Three-dimensional effects on flag flapping dynamics," *J. Fluid Mech.*, vol. 783, pp. 103–136, 2015.

[12] D. Akcabay and Y. Young, "Hydroelastic response and energy harvesting potential of flexible piezoelectric beams in viscous flow," *Phys. Fluids*, vol. 24, p. 054106, 2012.

[13] O. Doare and S. Michelin, "Piezoelectric coupling in energy-harvesting fluttering flexible plates: linear stability analysis and conversion efficiency," *J. Fluids Struc.*, vol. 27, pp. 1357–1375, 2013.

[14] S. Michelin and O. Doare, "Energy harvesting efficiency of piezoelectric flags in axial flows," *J. Fluid Mech.*, vol. 714, pp. 489–504, 2013.

[15] D. Kim, J. Cosse, C. Cerdeira, and M. Gharib, "Flapping dynamics of an inverted flag," *J. Fluid Mech.*, vol. 736, p. R1, 2013.

[16] K. Shoele and R. Mittal, "Energy harvesting by flow-induced flutter in a simple model of an inverted piezoelectric flag," *J. Fluid Mech.*, vol. 790, pp. 582–606, 2016.

[17] X. Wang, S. Alben, C. Li., and Y. Young, "Stability and scalability of piezoelectric flags," *Phys. Fluids*, vol. 28, p. 023601, 2016.

[18] S. Mazharmanesh, J. Young, F. Tian, S. Ravi, and J. Lai, "Energy harvesting of inverted piezoelectric flags in an oscillating flow," *J. Fluids Struc.*, vol. 115, p. 103762, 2022.

[19] X. Bi, C. Wang, Q. Zhu, and H. Tang, "Energy harvesting using an inverted piezohydroelastic flag with resistor-inductor-capacitor circuit," *J. Fluid Mech.*, vol. 975, p. A49, 2023.

[20] S. Lim and S. Park, "Numerical analysis of energy harvesting system including an inclined inverted flag," *Phys. Fluids*, vol. 34, p. 013601, 2022.

[21] X. Xie, Q. Wang, and N. Wu, "Potential of a piezoelectric energy harvester from sea waves," *J. Sound. Vib.*, vol. 333, pp. 1421–1429, 2014.

[22] Y. Cui, H. Wang, M. Li, and K. Sun, "Simulation of wave energy harvesting by piezoelectric seaweed," *IOP Conf. Ser: Mater. Sci. Eng.*, vol. 250, p. 012022, 2017.

[23] N. Wang, J. Zou, Y. Yang, X. Li, Y. Guo, C. Jiang, X. Jia, and X. Cao, "Kelp-inspired biomimetic triboelectric nanogenerator boosts wave energy harvesting," *Nano Energy*, vol. 55, pp. 541–547, 2019.

[24] Y. Wang, X. Liu, Y. Wang, H. Wang, H. Wang, S. Zhang, T. Zhao, M. Xu, and Z. Wang, "Flexible seaweed-like triboelectric nanogeerator ad a wave energy harvester powering marine internet of things," *ACS Nano*, vol. 15, no. 10, pp. 15700–15709, 2021.

[25] D. Goldstein, R. Handler, and L. Sirovich, "Modelling a no-slip flow boundary with an external force field," *J. Comput. Phys.*, vol. 105, pp. 354–366, 1993.

[26] K. Shoele and Q. Zhu, "Leading edge strengthening and the propulsion performance of flexible ray fins," *J. Fluid Mech.*, vol. 693, pp. 402–432, 2012.

[27] K. Kim, S. Baek, and H. Sung, "An implicit velocity decoupling procedure for the incompressible navier–stokes equations," *Int. J. Numer. Meth. Fluids*, vol. 38, pp. 125–138, 2002.

[28] K. Shoele and Q. Zhu, "Performance of a wing with nonuniform flexibility in hovering flight," *Phys. Fluids*, vol. 25, p. 041901, 2013.

[29] Y. Xia, S. Michelin, and O. Doare, "Fluid-solid-electric lock-in of energy harvesting piezoelectric flags," *Phys. Rev, Appl.*, vol. 3, p. 014009, 2015.

[30] T. Tan and Z. Yan, "Electromechanical decoupled model for cantilever-beam piezoelectric energy harvesters with inductive-resistive circuits and its application in galloping mode," *Smart Mater. Struct.*, vol. 26, p. 035062, 2017.